Arab J Sci Eng (2014) 39:9093–9100
DOI 10.1007/s13369-014-1456-1

RESEARCH ARTICLE - MECHANICAL ENGINEERING

Flow Behavior of Lead-Free Machinable Brass During Hot Compression Deformation

Gan Chunlei · Zheng Kaihong · Wang Haiyan · Qi Wenjun · Zhou Nan

Received: 30 June 2014 / Accepted: 30 September 2014 / Published online: 9 November 2014

Abstract Hot compression tests were carried out to study the deformation behaviors of a lead-free machinable brass using Gleeble-1500 thermal simulator in the temperature range of 823–973 K and the strain rate range of 0.01–10 s^{-1}. The results show that the flow behavior of the lead-free machinable brass is strongly influenced by strain rate and temperature, and the flow stress increases with increasing strain rate and decreasing temperature. The constitutive equations incorporating the effects of strain rate and temperature have been established to model the hot deformation behavior of this alloy. The reliability of the developed constitutive model was demonstrated by the mean percentage error of 10.82 % and the correlation coefficient of 0.98. Moreover, the flow stability/instability of the lead-free machinable brass was carefully investigated on the basis of dynamic material modeling approach. It was found that plastic deformation was stable for processing conditions in which the strain rate range was 1–10 s^{-1} within the temperature range of 823–923 K.

Keywords Lead-free machinable brass · Hot compression deformation · Flow behavior · Constitutive model

الخلاصة

لقد أجريت اختبارات الضغط الساخن لدراسة سلوكيات التشوه من النحاس المشكل الخالي من الرصاص باستخدام محاكاة جليبل-1500 الحرارية في درجات حرارة تتراوح بين 823-973 كيلفن ونطاق معدل إجهاد من0.01-10 / ثانية. وبينت النتائج أن سلوك تدفق النحاس المشكل الخالي من الرصاص يتأثر بشدة بمعدل الإجهاد ودرجة الحرارة ، ويزداد التوتر مع زيادة معدل تدفق الإجهاد وخفض درجة الحرارة. وتم إنشاء المعادلات التأسيسية المتضمنة لآثار معدل الإجهاد ودرجة الحرارة لنمذجة سلوك التشوه الساخن من هذه السبائك. وقد أثبتت موثوقية النموذج التأسيسي المطور من خلال متوسط خطأ نسبي من 10.82٪ ومعامل ارتباط من 0.98. وعلاوة على ذلك، فقد تم التحقيق في استقرار / عدم استقرار تدفق النحاس المشكل الخالي من الرصاص بعناية على أساس نهج نمذجة المواد الديناميكي. وقد وجد أن تشوه البلاستيك كان مستقراً لظروف المعالجة التي تضمنت نطاق معدل الإجهاد من 1-10 / ثانية ضمن درجات حرارة تتراوح بين 823-923 كيلفن.

1 Introduction

Lead-free machinable brasses have attracted great attentions at various industries due to the growing environmental concerns. Development of easily machinable lead-free brass has been considered by many researchers [1–4]. However, different deformation behaviors of this series of alloys may easily cause the defects of microstructure and property after hot deformation, which can limit the further development of these materials. Therefore, it is necessary to understand hot deformation behavior and flow characteristic of this series of alloys in more details. So far, great attention is given to study machinability, tensile properties and corrosion properties of lead-free machinable brasses in the current scientific literature [5–7]. However, there is still a lack of in-depth knowledge on the high temperature flow behavior of lead-free machinable brasses.

G. Chunlei (✉) · Z. Kaihong · W. Haiyan · Q. Wenjun · Z. Nan
Guangzhou Research Institute of Non-ferrous Metals, Guangzhou 510650, China
e-mail: ganchunlei@163.com

Flow behavior of materials during hot deformation processes is rather complex, because it is significantly affected by various working parameters such as the deformation degree, temperature and strain rate [8–10]. Hence, the understandings of hot deformation behavior of metals or alloys are of vital importance for designing the forming processes. The constitutive relation which can relate the flow stress, strain rate and temperature may generally be used to describe the plastic flow behaviors of metals or alloys. The constitutive model was capable to predict and characterize the flow behavior of materials in different regions of the hot compression stress–strain curves which included work hardening, dynamic recovery, dynamic recrystallization and flow instability [11]. Investigation on the flow behavior of lead-free machinable brasses at elevated temperatures is thus essential for optimization of the hot working process.

The main objective of this study was to evaluate the flow behavior of the lead-free machinable brass by hot compression tests under various deformation conditions. Based on the experimental data, constitutive equations for the flow stress dependence on strain rate and temperature are applied to describe the plastic flow property of the material. The reliability of the constitutive equation is assessed by the mean error of the peak flow stress between the predicted and experimental results. The flow stability was also investigated using a dynamic material modeling approach. The results will provide useful guidelines for the optimization of processing parameters of this lead-free machinable brass.

2 Material and Experimental Procedure

2.1 Material

The material used in this study is newly developed in our lab, and its nominal chemical composition (wt%) is Cu–36.3Zn–1.76Mg–0.5Bi–0.5Sb. In addition, the original microstructure of the as-received lead-free brass consisting of α phase, β phase and machinable particles is exhibited in Fig. 1.

2.2 Experimental Procedures

The hot compression tests were conducted on a Gleeble-1500 thermal simulator in the strain rate range of 0.01–10 s^{-1} and the temperatures range of 823–973 K. Cylindrical specimens with 15 mm height and 10 mm diameter were prepared to carry out compression tests. In order to minimize the friction between the specimen and die during hot deformation, the flat ends of the specimen were recessed to a depth of 0.2 mm deep to entrap the lubricant of graphite mixed with machine oil, as shown in Fig. 2. The specimens prior to isothermal compression were heated to the designed temperature and held for 3 min in order to obtain a homogeneous heat distribution. The reduction in height is 60 % at the end of the compression tests. During preheating and testing, a positive argon gas pressure was maintained in the heating chamber to avoid oxidation.

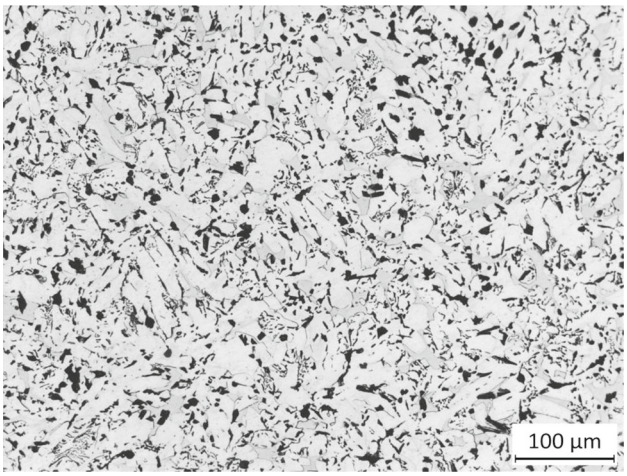

Fig. 1 Microstructure of the as-received lead-free machinable brass

Fig. 2 Typical appearance of the specimens of the lead-free machinable brass before the hot compression tests

3 Results and Discussion

3.1 Flow Behavior

Typical true stress–true strain curves obtained from the hot compression tests of the lead-free machinable brass in a wide range of deformation temperature and strain rate conditions are depicted in Fig. 3. As is seen, the flow stress level is significantly affected by the temperature and strain rate. The flow stress decreases with the increase in temperature and the decrease in strain rate. Meanwhile, the flow curves exhibit the obvious flow softening phenomena. The

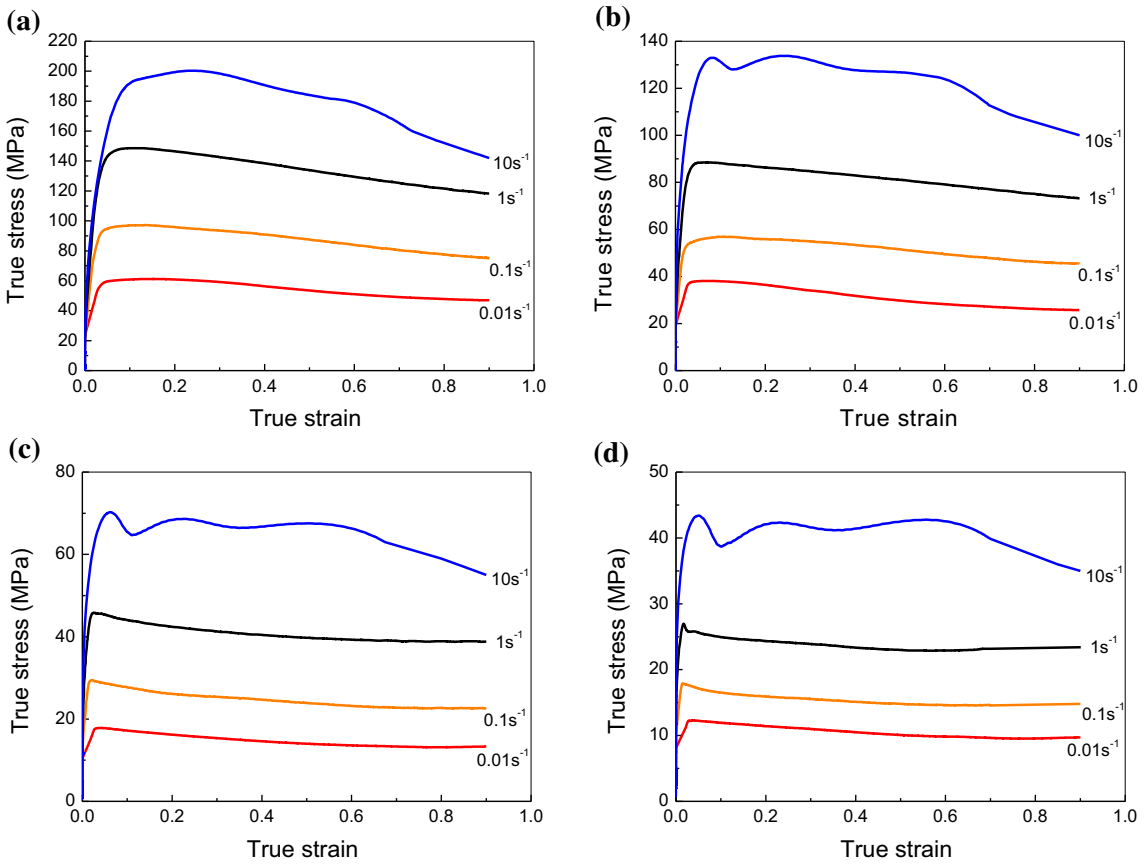

Fig. 3 True stress–true strain curves for the lead-free machinable brass alloy under different deformation temperatures. **a** 823 K, **b** 873 K, **c** 923 K, **d** 973 K

higher the deformation temperature and the lower the strain rate, the greater the flow softening tendency becomes. The cause can lie in the fact that the higher temperature and lower strain rate promote the higher mobility of grain boundary and growth of dynamically recrystallized grains. The peak stresses on the true stress–strain curves further suggest that the dynamic recrystallization and dynamic flow softening of the lead-free machinable brass occurs during hot compression.

3.2 Constitutive Analysis of the Flow Stress

Based on these flow curves obtained in the hot compression tests, a material constitutive equation was developed to further understand the plastic flow behavior of the experimental lead-free machinable brass. To formulate the constitutive equation of the alloy, the Arrhenius equation which was widely used to describe the relationship between the strain rate, temperature and flow stress was utilized in this study [12–14]. Three types of Arrhenius equations are shown as follows:

$$\dot{\varepsilon} = A\sigma^{n_1} \exp\left(-Q/R_0T\right) \tag{1}$$

$$\dot{\varepsilon} = A \exp\left(\beta_1\sigma\right) \exp\left(-Q/R_0T\right) \tag{2}$$

$$\dot{\varepsilon} = A \left[\sinh\left(\alpha_0\sigma\right)\right]^n \exp\left(-Q/R_0T\right) \tag{3}$$

where R_0 denotes the universal gas constant (8.314 J mol^{-1} K^{-1}), $\dot{\varepsilon}$ is strain rate (s^{-1}), σ is the flow stress (MPa) for a given true stain, Q is the deformation activation energy (kJ mol^{-1}) and T is temperature (K). β_1, n_1, α_0, n and A are the material constants, where $\alpha_0 = \beta_1/n_1$. It is worth to say that since the peak stress is more commonly applied due to easy identifiability on the flow curve [15], σ is considered to be the peak flow stress in the present study. It has been reported that Eqs. (1)–(3) are the most frequently used equations describing the thermally activated process during hot deformation. Equations (1) and (2) are suitable for low stress regime (i.e., $\alpha_0\sigma < 0.8$) and high stress regime (i.e., $\alpha_0\sigma > 1.2$), respectively, whereas Eq. (3) is a more general form which can be applied to stresses over a wider range. Because Eq. (3) is found to be more representative and most suitable form for explaining the deformation behavior, the hyperbolic sine law equation was applied in the present work.

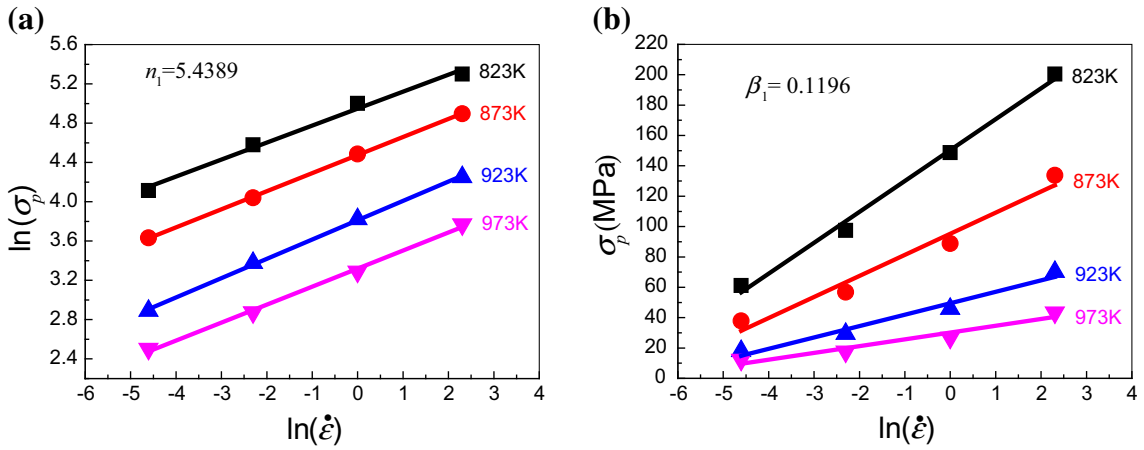

Fig. 4 Relationships between **a** ln $(\dot{\varepsilon})$ and ln(σ_p); **b** ln $(\dot{\varepsilon})$ and σ_p

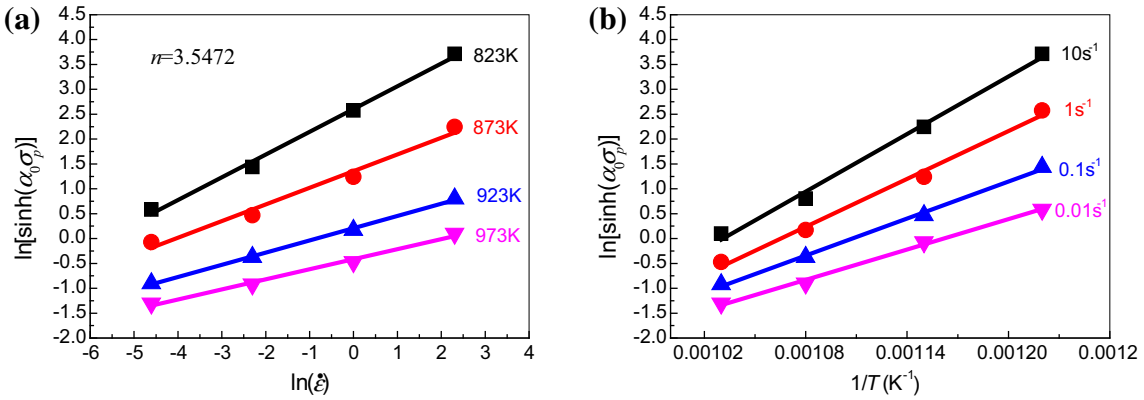

Fig. 5 Evaluating the values of **a** n by fitting ln[sinh$(\alpha_0\sigma_p)$] − ln $(\dot{\varepsilon})$ and **b** Q by fitting ln[sinh$(\alpha_0\sigma_p)$] − $1/T$

3.2.1 Determination of Material Parameters for Hot Deformation Conditions

The true stress–strain data obtained from compression tests under different strain rate and temperature conditions were used to determine the material constant of the aforementioned constitutive equation. To achieve this purpose, the flow stress value at the curve maximum is taken as an example for demonstrating solution procedure of the involved material constants.

For low and high stress levels, Eqs. (1) and (2) result in the following relationships, respectively:

$$\ln \dot{\varepsilon} = n_1 \ln \sigma_p + \ln A - Q/R_0T \tag{4}$$

$$\ln \dot{\varepsilon} = \beta_1 \sigma_p + \ln A - Q/R_0T \tag{5}$$

Taking the partial differentiation of Eqs. (4) and (5) with respect to the peak flow stress (σ_p) at constant temperature, one would get

$$\left[\frac{\ln(\sigma_p)}{\ln \dot{\varepsilon}}\right]_T = \frac{1}{n_1} \tag{6}$$

$$\left[\frac{\sigma_p}{\ln \dot{\varepsilon}}\right]_T = \frac{1}{\beta_1} \tag{7}$$

Figure 4a, b shows that the values of $1/n_1$ and $1/\beta_1$ are obtained from the slope of the lines in the plots of ln (σ_p) − ln $(\dot{\varepsilon})$ and σ_p − ln $(\dot{\varepsilon})$. The mean value of the slopes was considered as the values of n_1 and β_1, which was found to be 5.4389 and 0.1196 MPa, respectively. This gives the value of $\alpha_0 = \beta_1/n_1 = 0.02199\ \text{MPa}^{-1}$.

For the whole stress values including low and high stress levels, taking the logarithm on both sides of the above Eq. (3) gives

$$\ln\left[\sinh\left(\alpha_0\sigma_p\right)\right] = \frac{1}{n}\ln \dot{\varepsilon} + \frac{Q}{nR_0T} - \frac{1}{n}\ln A \tag{8}$$

At a constant temperature during the hot deformation process, the value of n can be acquired by making a liner fitting of ln[sinh$(\alpha_0\sigma_p)$] − ln $(\dot{\varepsilon})$, that is:

$$\left[\frac{\partial \ln\left[\sinh\left(\alpha_0\sigma_p\right)\right]}{\partial\left(\ln \dot{\varepsilon}\right)}\right]_T = \frac{1}{n} \tag{9}$$

Table 1 Determined materials parameters for the lead-free machinable brass

Material	α_0 (MPa^{-1})	n	Q (kJ/mol)	A (s^{-1})
Lead-free machinable brass	0.02199	3.5472	426.817 ± 20	3.4307×10^{23}

From a group of parallel and straight lines in Fig. 5a, it can be easily evaluated for the n-values, by averaging the values of n under different temperatures. The average of n value was found to be 3.5472. In the same way, for a particular strain rate, differentiating Eq. (8) gives

$$\left[\frac{\partial \ln\left[\sinh\left(\alpha_0\sigma_p\right)\right]}{\partial\left(T^{-1}\right)}\right]_{\dot{\varepsilon}} R_0 n = Q \tag{10}$$

Equation (10) gives the value of Q from the variations of flow stress with strain rate and temperature according to the hyperbolic sine function. Therefore, by substituting the values of temperatures and flow stresses obtained at fixed strain rate into Eq. (10), the value of Q can be derived from the slope of plotting $\ln[\sinh(\alpha_0\sigma_p)]$ as a function of $1/T$, as shown in Fig. 5b. It can be seen that the linear correlation between $\ln[\sinh(\alpha_0\sigma_p)]$ and $1/T$ is relatively high; thus, the value of activated energy (Q) can be obtained as 426.817 ± 20 kJ/mol.

Since the value of Q has been obtained, it is easy to evaluate the value of the material constant A in Eq. (7) to be 3.4307×10^{23} s^{-1} according to the linear regression of the $\ln[\sinh(\alpha_0\sigma_p)] - \ln(\dot{\varepsilon})$ plots at each temperature as shown in Fig. 5a.

Table 1 shows the calculated values of all material parameters required for the flow stress prediction of the lead-free machinable brass. It was found that the activation energy of 426.817 ± 20 kJ/mol was similar to those reported values of other copper based alloys, in which the activation energies were typically in the range of 214–572 kJ/mol [16–18].

3.2.2 Comparison of the Peak Flow Stresses

In order to test the adequacy of the developed equation, a comparison between the measured and predicted results from the above-mentioned computation is carried out. According to Eq. (3) at constant temperature and strain rate, a general expression for the peak flow stress can be written as

$$\sigma_p = \frac{1}{\alpha_0}\ln\left\{\left(\dot{\varepsilon}\exp\left(\frac{Q}{R_0T}\right)/A\right)^{1/n} + \left[\left(\dot{\varepsilon}\exp\left(\frac{Q}{R_0T}\right)/A\right)^{2/n} + 1\right]^{1/2}\right\} \tag{11}$$

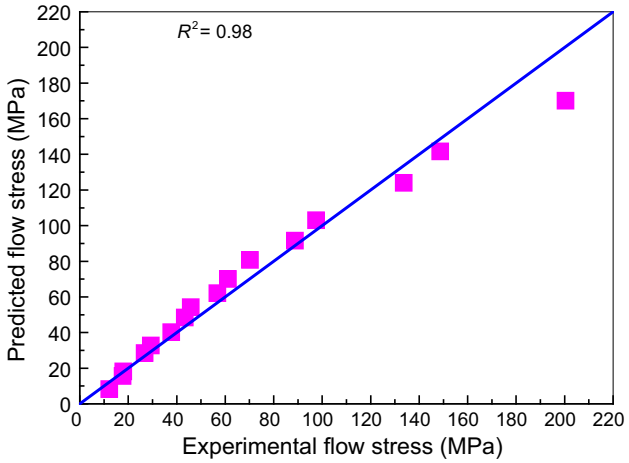

Fig. 6 Correlation between the experimental and predicted peak flow stresses data from the developed constitutive equation of the lead-free machinable brass alloy

When the values of material constants from Table 1 are substituted into Eq. (11), the following expression to predict peak flow stress of the investigated lead-free machinable brass at a given temperature and strain rate can be obtained:

$$\sigma_p = \frac{1}{0.02199}\ln\left\{\left(\frac{\dot{\varepsilon}\exp\left(\frac{426{,}817}{R_0T}\right)}{3.4307\times10^{23}}\right)^{1/3.5472} + \left[\left(\frac{\dot{\varepsilon}\exp\left(\frac{426{,}817}{R_0T}\right)}{3.4307\times10^{23}}\right)^{2/3.5472} + 1\right]^{1/2}\right\} \tag{12}$$

The comparison of the measured and predicted peak flow stresses by Eq. (12) under all the experimental conditions is shown in Fig. 6. In most cases, the predicted flow stresses show a high agreement with the experimental flow stresses at lower rates compared with those at higher rates. The mean percentage error of all peak flow stresses shown in Fig. 6 is 10.82 % with the square of the correlation coefficient $R^2 = 0.98$. This suggests that the proposed deformation constitutive model can agree well with the experimental values and can be employed to analyze the flow behavior during the hot forming process of the lead-free machinable brass.

4 Flow Stability During Hot Deformation

It has shown that the hot flow behavior of the investigated lead-free machinable brass is obviously sensitive to strain rate and temperature. For example, an increase of strain rate greatly enhances the flow stress, whereas the flow stress is apparently decreased due to an increase in temperature. At higher deformation rate, large amount of heat is often pro-

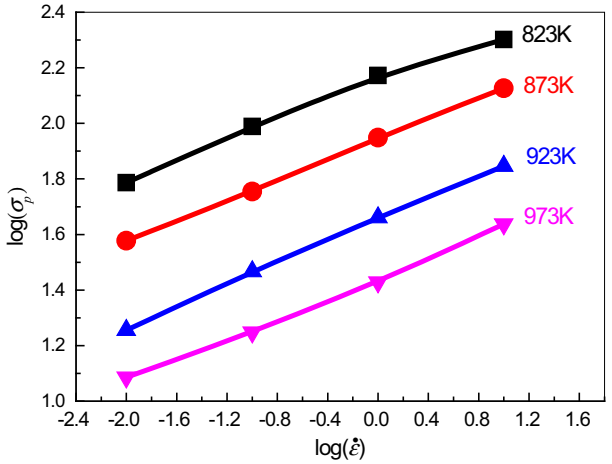

Fig. 7 Evaluating the value of m by plotting log σ_p versus log ($\dot{\varepsilon}$)

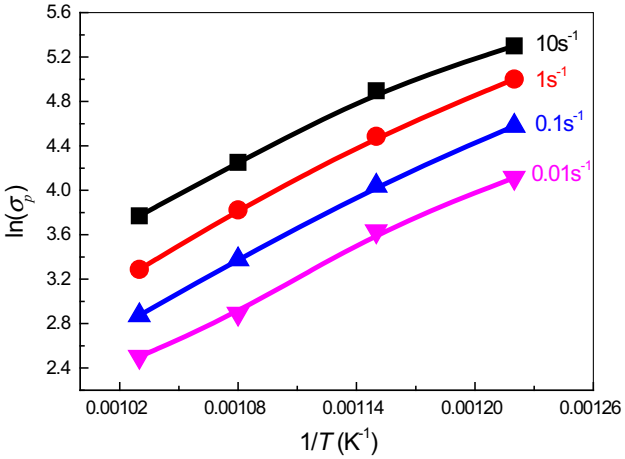

Fig. 8 Evaluating the value of n by plotting ln(σ_p) versus 1/T

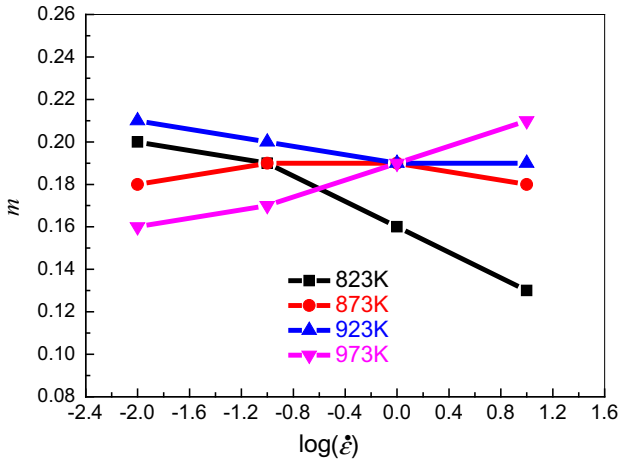

Fig. 9 The strain rate sensitivity m versus log ($\dot{\varepsilon}$) at different temperatures

duced. As a result, the material exhibits flow softening behavior and ultimately material instability can occur. Dynamic material modeling [19–21] was widely used to characterize the deformation behavior. This method has been successful in correlating flow stability/instability condition and the plastic flow behavior through the strain rate sensitivity m and the temperature sensitivity s at specific temperature and strain rate. In order to effectively evaluate the flow stability of the lead-free machinable brass during hot deformation, the dynamic material modeling stability criteria developed by Malas and Seetharaman [22] were used in the present study.

In terms of the principles of the dynamic material modeling, the plastic stable zones can be established during the steady energy dispersion processes, if and only if the following four criteria are met for stable flow simultaneously:

$$0 < m < 1 \tag{13}$$

$$\frac{\partial m}{\partial(\log \dot{\varepsilon})} \leq 0 \tag{14}$$

$$s > 1 \tag{15}$$

$$\frac{\partial s}{\partial(\log \dot{\varepsilon})} \leq 0 \tag{16}$$

where the strain rate sensitivity $m = [\partial \log(\sigma_p)/\partial \log \dot{\varepsilon}]_T$ can be determined from the slopes of the flow peak stress versus strain rate at different temperatures as shown in Fig. 7, and the temperature sensitivity $s = 1/T[\partial \log(\sigma_p)/\partial(1/T)]_{\dot{\varepsilon}}$ can be obtained according to the slopes of the $\ln(\sigma_p)$ versus $1/T$ graph at different temperatures as shown in Fig. 8. The two material parameters are considered to be related to the manner of the energy dispersion during hot deformation.

The strain rate sensitivity m is an important material property, which can significantly influence hot workability of metals or alloys. Figure 9 shows the variation of m versus the strain rate at given temperatures. It could be found that the strain rate sensitivity m varied from 0.13 to 0.21 and hence the criterion in Eq. (13) was always satisfied for all temperatures and strain rates. However, the rate of change of m with respect to log ($\dot{\varepsilon}$) is relatively complex. The rate of change of m was always negative or equal to zero for the temperatures of 823 and 873 K in the strain rate range of 0.01–10 s^{-1}, which implied that the criterion in Eq. (14) was fully satisfied. For the temperature of 923 K, the criterion in Eq. (14) was not satisfied in the strain rate range of 0.01–0.1 s^{-1}, whereas the criterion was enough satisfied in the strain rate range of 0.1–10 s^{-1} due to the negative or zeroth rate of change of m. When the temperature was further increased to 973 K, the rate of change of m was always positive for all strain rates and hence the criterion in Eq. (14) was not satisfied. This indicated that material instability might occur during hot deformation.

The other important factor affecting hot deformation behavior is the temperature sensitivity s in Eq. (15), which indicates that the rate of net entropy production is always positive as required for stable flow conditions in an irreversible process [23]. The variation of s versus the strain rate for

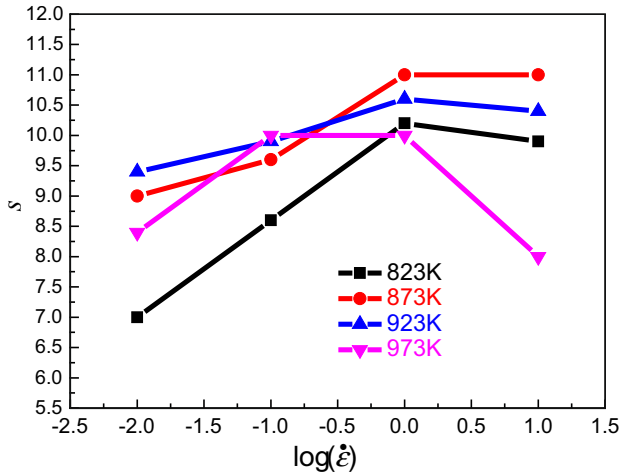

Fig. 10 The temperature sensitivity s versus log $(\dot{\varepsilon})$ at different temperatures

Table 2 Conditions of satisfaction for each criterion according to dynamic material modeling approach for the lead-free machinable brass

Criteria	T (K)	$\dot{\varepsilon}$ (0.01−0.1 s^{-1})	$\dot{\varepsilon}$ (0.1−1 s^{-1})	$\dot{\varepsilon}$ (1−10 s^{-1})
$0 < m < 1$	823–973	○	○	○
$\frac{\partial m}{\partial(\log \dot{\varepsilon})} \leq 0$	823–873	×	○	○
	873–923	×	○	○
	923–973	×	×	×
$s > 1$	823–973	○	○	○
$\frac{\partial s}{\partial(\log \dot{\varepsilon})} \leq 0$	823–873	×	×	○
	873–923	×	×	○
	923–973	×	×	○

The symbols such as "○" and "×" denote satisfied or unsatisfied condition for each criterion

different temperatures is plotted in Fig. 10. It is clear that the temperature sensitivity s varied from 7 to 11 and hence the criterion in Eq. (15) was always satisfied for the entire experimental range. However, the rates of change of the temperature sensitivity s with respect to log $(\dot{\varepsilon})$ were positive for the strain rate range of 0.01–1 s^{-1} within the temperature range of 823–923 K and the strain rate range of 0.01–0.1 s^{-1} at the temperature of 973 K. These deformation conditions did not satisfy the criterion in Eq. (16). Only when the strain rate range was 1–10 s^{-1} within the temperature range of 823–923 K and the strain rate range of 0.1–10 s^{-1} for the temperature of 973 K, the criterion in Eq. (16) was satisfied.

The state of satisfaction for each criterion at different range of temperatures and strain rates is further summarized in Table 2. It has been known that only when all four criteria of the dynamic material modeling are verified simultaneously, the flow stability can be determined. Therefore, it can be reasonably concluded that plastic deformation of the lead-free machinable brass is stable at strain rates between 1 and 10 s^{-1} and the temperature range of 823–923 K.

5 Conclusions

The hot deformation behaviors of the lead-free machinable brass were investigated by the compression tests in the temperature range of 823–973 K and the strain rate range of 0.01–10 s^{-1}. The main conclusions can be obtained as follows:

1. The flow behavior strongly depends on strain rate and temperature, and the flow stress increases with the increase of strain rate and the decrease of temperature.
2. On the basis of the experimental data from the hot compression tests, the material constants (i.e., α_0, n, Q and A) of the Arrhenius equation with hyperbolic sine law were obtained. The activation energy Q for the investigated strain rate and temperature ranges was 426.817 ± 20 kJ/mol, which was in reasonable agreement with copper alloys reported before.
3. The constitutive equation incorporating the effects of temperature and strain rate was developed to describe the flow stress behavior of the lead-free machinable brass. The high correlation coefficient ($R^2 = 0.98$) and the mean percentage error (10.82 %) for the flow stress obtained from the established model indicate that the model can be used to numerically simulate the hot deformation behavior of the lead-free machinable brass.
4. Dynamic material modeling can be effectively utilized to summarize flow stability/instability of the lead-free machinable brass. In the investigated range, the optimal conditions for hot working of this alloy can be the strain rate range of 1–10 s^{-1} and between 823 and 923 K, where the plastic flow is considered to be stable.

Acknowledgments The financial supports received for this study from the PhD start-up fund of Guangzhou Research Institute of Nonferrous Metals (No. 2012B001), University-industry Cooperation Project of Guangzhou (No. 7411804513611) and Ministry of Education of Guangdong Province University-industry Cooperation Project (No. 2012B091100038) are gratefully acknowledged.

References

1. Toshikazu, M.; Takayuki, O.: Cutting of lead-free copper alloy "Eco Brass". J. Jpn. Res. Inst. Adv. Copper Base Mater. Technol. **45**, 250–255 (2006)
2. Emelina, N.B.; Alabin, A.N.; Belov, N.A.: Influence of Bismuth and Lead on the formation of the structure of experimental alloys with a Cu-30%Zn based composition during crystallization, deformation, and thermal treatment. Russ. J. Non Ferrous Metals **51**, 476–482 (2010)

3. Li, S.F.; Kondoh, K.; Imai, H.; Atsumi, H.: Fabrication and properties of lead-free machinable brass with Ti additive by powder metallurgy. Powder Technol. **205**, 242–249 (2011)
4. Mohamed, A.T.; Nahed, A.E.; Rawia, M.H.; Tarek, M.M.; Mohamed, H.G.: Machinability characteristics of lead free-silicon brass alloys as correlated with microstructure and mechanical properties. Ain Shams Eng. J. **3**, 383–392 (2012)
5. You, S.J.; Choi, Y.S.; Kim, J.G.; Oh, H.J.; Chi, C.S.: Stress corrosion cracking properties of environmentally friendly unleaded brasses containing bismuth in Mattsson's solution. Mater. Sci. Eng. A **345**, 207–214 (2003)
6. Xiao, L.R.; Shu, X.P.; Yi, D.Q.; Zhang, X.M.; Qin, J.L.; Hu, J.R.: Microstructure and properties of unleaded free-cutting brass containing stibium. Trans. Nonferrous Metals Soc. China **17**, 1055–1059 (2007)
7. Atsumi, H.; Imai, H.; Li, S.F.; Kondoh, K.; Kousaka, Y.; Kojima, A.: High-strength, lead-free machinable-duplex phase brass Cu–40Zn–Cr–Fe–Sn–Bi alloys. Mater. Sci. Eng. A **529**, 275–281 (2011)
8. Al-Dheylan, K.; Hafeez, S.: Tensile failure micromechanisms of 6061 aluminum reinforced with submicron Al_2O_3 metal-matrix composites. Arab. J. Sci. Eng. **31**, 89–98 (2006)
9. Pilehva, F.; Zarei-Hanzaki, A.; Ghambari, M.; Abedi, H.R.: Flow behavior modeling of a Ti–6Al–7Nb biomedical alloy during manufacturing at elevated temperatures. Mater. Design **51**, 457–465 (2013)
10. Li, H.Z.; Wang, H.J.; Li, Z.; Liu, C.M.; Liu, H.T.: Flow behavior and processing map of as-cast Mg–10Gd–4.8Y–2Zn–0.6Zr alloy. Mater. Sci. Eng. A **528**, 154–160 (2010)
11. Thossatheppitak, B.; Uthaisangsuk, V.; Mungsuntisuk, P.; Suranuntchai, S.; Manonukul, A.: Flow behaviour of nickel aluminium bronze under hot deformation. Mater. Sci. Eng. A **604**, 183–190 (2014)
12. Zencer, C.; Hollomon, J.H.: Effect of strain rate upon plastic flow of steel. J. Appl. Phys. **15**, 22–32 (1944)
13. Wu, B.; Li, M.Q.; Ma, D.W.: The flow behavior and constitutive equations in isothermal compression of 7050 aluminum alloy. Mater. Sci. Eng. A **542**, 79–87 (2012)
14. Feng, W.; Fu, Y.H.: High temperature deformation behavior and constitutive modeling for 20CrMnTiH steel. Mater. Design **57**, 465–471 (2014)
15. Banerjee, S.; Robi, P.S.; Srinivasan, A.; Kumar, L.P.: High temperature deformation behavior of Al–Cu–Mg alloys micro-alloyed with Sn. Mater. Sci. Eng. A **527**, 2498–2503 (2010)
16. Ding, Z.Y.; Jia, S.G.; Zhao, P.F.; Deng, M.; Song, K.X.: Hot deformation behavior of Cu–0.6Cr–0.03Zr alloy during compression at elevated temperatures. Mater. Sci. Eng. A **570**, 87–91 (2013)
17. Xiao, Y.H.; Guo, C.; Guo, X.Y.: Constitutive modeling of hot deformation behavior of H62 brass. Mater. Sci. Eng. A **528**, 6150–6158 (2011)
18. Ji, G.L.; Li, Q.; Li, L.: The kinetics of dynamic recrystallization of Cu–0.4Mg alloy. Mater. Sci. Eng. A **586**, 197–203 (2013)
19. Menon, S.S.; Rack, H.J.: Flow stability of binary Al–Li alloys. Mater. Sci. Eng. A **297**, 244–255 (2001)
20. Long, M.; Rack, H.J.: Thermo-mechanical stability of forged Ti–26Al–10Nb–3V–1Mo (at.%). Mater. Sci. Eng. A **194**, 99–111 (1995)
21. Bruschi, S.; Poggio, S.; Quadrini, F.; Tata, M.E.: Workability of Ti–6Al–4V alloy at high temperatures and strain rates. Mater. Lett. **58**, 3622–3629 (2004)
22. Malas, J.C.; Seetharaman, V.: Using material behavior models to develop process control strategies. J. Metals **44**, 8–13 (1992)
23. Dieter, G.E.; Kuhn H.A.; Semiatin S.L.: Handbook of Workability and Process Design. ASM International, Materials Park, OH, pp. 17–19 (2003)